Caracterization of the skin.

Ourkiya Maison Loukkas Lindor Krimech Chan

In this paper, a system, consisting a sensor mounted on a rotating axe around a stepper motor in order to calculate a polar diffusion diagram of skin sample which is based on its reflectance rate, is presented. Moreover, a spectrophotometer is used to gather the data of the tissue as a spectrum in visible wavelengths. Once, signal-to-noise ratio computation is performed, its data feed a processing system to characterize each sample and then, a cross-validated recognition task, achieving 100% accuracy and legitimizing the biometric application of this method, is executed.

1. Introduction

Skin is the largest organ of the body and the most discriminative part of the recognition task of different human beings. Its inner characteristics of humidity determines the quality of the skin pores [1], and the skin chromophores constitutes the main element of interaction with light [2]–[4]. The melanin rate is used to make a barrier to avoid harmful exposure of electromagnetic radiations in the environment [5], and the oxy-hemoglobin which can be found in veins can inform suffocation or breath irregularities of the human being [6]. Moreover, the blood flow can be analyzed in order to determine the heartbeat of the body, among other uses [7]. The skin has very specific properties studied in different fields as in cosmetics (how to make more efficient products that penetrate the skin/protect it [8]), computer graphics (in order to emulate realistic tissues [9]), and medicine to evaluate irregularities of the skin, and human health [10].

Optical Analysis of human skin is a non-invasive way to observe skin physiology, morphology and composition. For instance, white light can be used to obtain a spectrum which is useful to analyze the skin and also all the quantitative variations related to skin components. Reflective properties are used to identify and recognize humans by presenting a part of their skins, as in biometrics, and to detect spatially distributed irregularities such as veins or abnormally vascularized regions, melanomas or malign tumors. In fact, different skin tissues have distinct or unique reflectance pattern which helps to differentiate different skin conditions [2], [11], [12]. Hence, the idea behind the diffuse reflectance is that light reflected from a target tissue provides information on the quantity of melanin pigment and its chemical structure, oxygenated and deoxygenated hemoglobin, carotene, and also the chemicals [13], [14]. This information, based on biochemical composition and the structure of the tissue, does not only indicate the presence and location of the pathology, but also indicates where the pathology has originated, also contributes to find the most appropriate treatment to cure the pathology by observing the characteristics of the tissue if it is needed [11], [12].

Those characteristics and the recent developments in analytical techniques of the skin, made us think about what kind of system should be envisaged to identify individuals in terms of biometrics. Thus, analyzing diffusion diagram of the skin, and the spectrum of skin diffusion by using certain wavelength is proposed.

In the first section different physical aspects of the interaction of light with skin are introduced. Then the measurement system is described and characterized. In the second section, samples, measurement protocol and results are presented. In the last section before conclusion, the obtained results are analyzed and discussed in terms of efficiency for biometric applications.

2. Development

   a. Physical aspects, skin-light interaction

Spectroscopy is a non-invasive method which allows to capture physiological and biochemical data of the tissue [15], [16]. Photons stream directed on the skin by a light source can be scattered, absorbed, reflected or transmitted. Skin contains various chromophores and rough surface [17]. Thus, light directed on skin tissue is affected by all above mentioned phenomena.

Each person has a different structure of skin, its thickness, distribution and capacity of various chromophores [3]. Therefore, input light directed on the skin is transformed in different ways for each person. Chromophores present in the skin, which have a major contribution to the light transformation, are hemoglobin, melanin, and others [11]. Each of them causes distinctive effects, which varies depending on the wavelength. The chromophores mainly absorb or scatter the incident light, while for water, lipids, and proteins, especially collagen, absorption is low and scatters high [18]. Melanin, which accumulates in basal layer of epidermis, is produced by melanocytes and is the sole pigment which affects the transmittance of human epidermis [5]. Melanin absorbs waves in spectrum between 250 and 1200 mm. The absorption intensity heightens towards shorter wavelengths and it is irregular. Consequently, most of short wavelengths opposite to the long ones are absorbed or retransmitted in epidermis and do not reach deeper skin layers [5]. Dermis optic features differ more from of
epidermis. The optics properties are determined by blood-borne chromophores - hemoglobin. It transports oxygen from lungs to the remaining tissues through blood vessels and returns carbon dioxide to lungs. The absorption of hemoglobin is present in spectral range of 390 nm to 1000 mm and has a few peaks depending whether the oxygen is transported. There are two peaks for hemoglobin without oxygen with maxima at 550 nm and 760 nm, and two with oxygen with maxima are at 548 nm and 576 nm [19].

Pathways of the incident light in skin are presented in Fig. 1 and absorption coefficient of different chromophores is representing as a function of wavelength in Fig.2, are summarizing, such a complex process of reflecting, scattering and absorbing of the electromagnetic radiation delivered by a light source, should affect the individual features of the skin spectra.

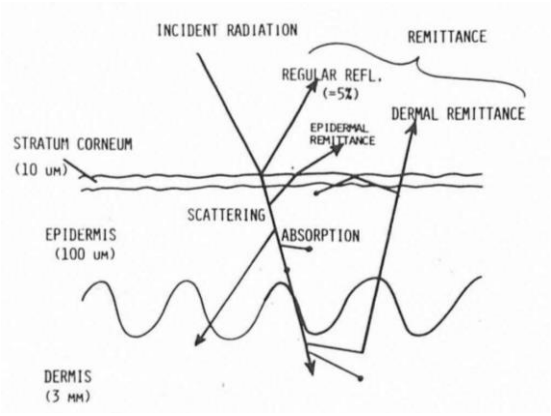

Fig.1 : Schematic diagram of optical pathways in human skin [11].

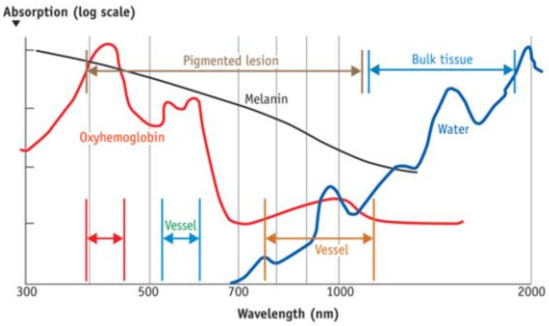

Fig.2: Absorption coefficients of different chromophores as a function of wavelengths, depending on the depth of light, and must be considered. [20]

Scattering relies upon coefficient a, height of the scattering center, the incident wavelength λ, and its angle Θ. In the Rayleigh model, the effective section for each solid angle is proportional to $\frac{a^6}{\lambda^4}(1+\cos^2\Theta)$. For bigger particles, a more relevant theory based on Mie's work supply intensity meters which are no longer isotropic, and the scattering takes places further as bigger the particle size rise [21].

The objective is to estimate the phase function $f(cos\Theta)$, or angular distribution of intensity of light that skin scatters. This phase function is a probability density, related to g, the anisotropic factor defined as $g = \int f(cos\Theta)cos\Theta\, d(cos\Theta)$, with $\Theta = \hat{s}.\hat{s}'$, angle between the incident direction of the wave, and direction of the scattered wave [21]. This anisotropic factor g quantifies anisotropic scattering, i.e. its inclination to be scattered in definite directions. Figure 3. summarizes those scattering theories (Rayleigh and Mie).

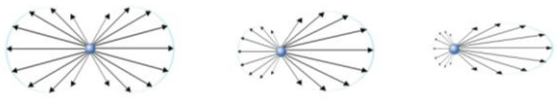
Fig.3: Radiation indicators for different kinds of scattering on a spheric particle, beam coming from left. Left, Rayleigh scattering; center, intermediate scattering (Rayleigh-Mie) ; right, Mie scattering, mostly forwards [22], [23].

For instance, $g = 0$ if scattering is perfectly isotropic, $g = 1$ if scattering is completely forwards (propagating without scattering). As a biological tissue, scattering goes forward in a general manner, with $0.8 < g < 0.98$. A certain amount still can scatter rearward, area of our experiment. The study consisted of variations of energetic parameters, function of the angle of view, represented in Figure 4.

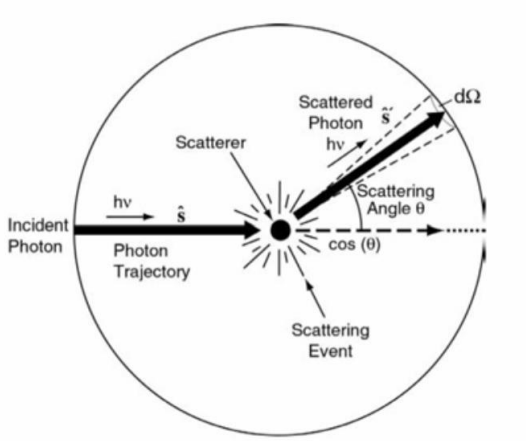

Fig.4: Definition of the incident direction $\hat{s}$, scattering trajectory $\hat{s}'$ and scattering angle. Credits: Tuan Vo-Dinh [23]

Thus, a sensible surface of a photodiode is placed perpendicular to the incident wave (approximately spherical) also in order to conserve invariant of solid angle for each measurement. For instance, if the captured luminance is measuring, the same solid angle will be obtained for each measurement while the photodiode surface is placing in a same way, tangentially at the front of spherical wave. The captured flux shows up with the same solid angle, therefore, coherent measurement is obtained with simple and fast calculations. The luminance in $W.m^{-2}.sr^{-1}$, which is pertinent and common parameter for our study, can be obtained, since the sensible surface of the sensor and solid angle are constant for each angle.

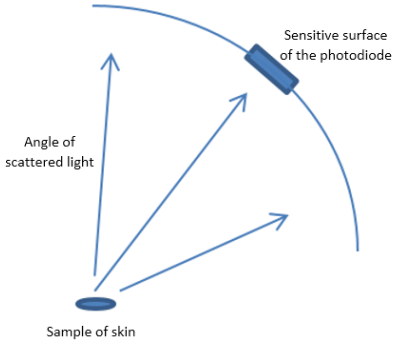

Fig. 5: Position of the photodiode

The choice of fixing the photodiode one extremity of mobile arm while the other extremity is relied on stepper motor. Fig. 5 shows the sweeping mechanism which is able to rotate at several angles, measures the diffusion for each different angle. Then the signal is transmitted into the acquisition chain.

b. Instrumental aspects

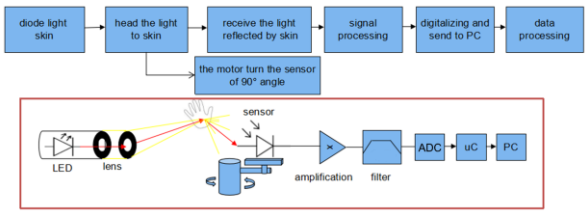

Fig.6: Descriptive diagram and schematic of the system, consisting of the photodiode mounted on stepper motor fixed in a box, in order to rotate the photodiode.

As it is seen in Fig. 6, the device is placed inside of a box in order to isolate the external light which can disturb the measurement. Light beam, emitted by LED and converging by lens in order to be focused on a skin sample. Photons stream, namely light beam, directed on the skin by a light source can be scattered, absorbed, reflected or transmitted. Reflected light, captured by the sensors, is converted into electrical current and amplified. A stepper motor on a mechanical arm is used in order to carry the sensor. This robotic arm is also providing rotational movement with several angles during the measurement. The signal, acquired by a sensor which is a photodiode, is sampled by the microcontroller, and is sent through a serial port to the computer. Saved and processed data is used as training example of a learning algorithm in order to develop a recognition tool.

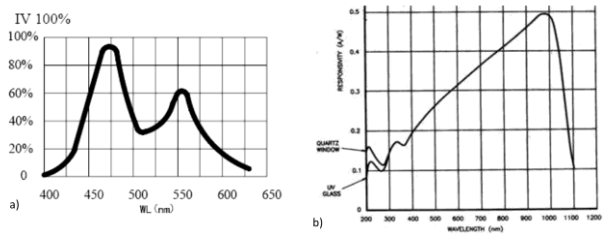

Fig.7: Spectral response of the emitting (a, 5050 LED) and receiving (b, OSD 35-7X CQ) components used for the experimentation.

A photodiode consists of an active p-n junction which is operated in reverse bias. When light falls on the junction, a reverse current flows which is proportional to the illuminance [25]. The linear response to light makes it an element in useful photodetectors for this applications. It is also used as the active element in light-activated switches. In Fig. 7, spectral response of photodiode is shown. Spectral response is a ratio of the generated photocurrent to incident light power, expressed in $A.W^{-1}$ when used in photoconductive mode. The wavelength dependence may also be expressed as a quantum efficiency, or the ratio of the number of photo generated carriers to incident photons [26].

Incident light emitted by LED, has a certain range of spectrum. The aim is to obtain the spectrum of light scattering as the output of the system. Incident light emitted by LED, has a certain spectrum. The skin absorbs some quantity of this incident light, which means the scattering, and reflect another part of the light. The reflected light is measured by a photodiode. Due to the characteristic of the photodiode, it is possible to capture certain band of frequency corresponds to the certain wavelength zone. In our case, a photodiode sensible to the near infra-red wavelengths [27], by minimizing environmental spectrum is minimized with closed environment in order to ignore it, is used. In fact, the measurand of the photodiode is current, and it is needed to be converted into voltage in order the make the data compatible with the micro controller which uses voltage as input unit. This photodiode voltage corresponds to the amount of photons filling potential wells, and is also correlated with the integration of the spectrum product into certain range of wavelengths.

c. Recognition system characteristics

Fig. 8: Illustration of the skin sample area (inside the red circle) used for each subjects, as input of the acquisition system.

Through the system described before, the photodiode sends a current for each step of the motor, and this current is converted to a digital number proportionally to its magnitude by an analog to digital converter (ADC). For each scanned skin sample from the back of hand of each subject, a dataset entry is created while the scan process is performing, and stored in order to use as an input of k-nearest neighbor based recognition system [28]. Those data are associated to spectrums acquired with an GretagMacbeth Eye-One spectrophotometer, which is already calibrated with white object as described in Fig. 9.

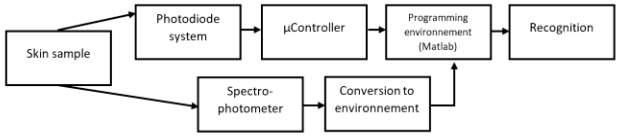

Fig. 9: Block-diagram of the recognition system. The skin sample is scanned at different time intervals in the system, and in the spectrophotometer.

When the dataset entry is created, several acquisitions have applied for the same angle, which is related to the position of stepper motor, calibrated with an offset, and calculated with turned off emitter, in the system as well as for the multiple entries of each wavelength spectrum with the spectrophotometer. This process permits to measure the means and the standard deviation for different acquisitions, which provides a model representing multiple presentations of the subject, through the statistical machine learning algorithm. It is important to emphasize that two process is differentiated, respectively learning phase, consisting

the acquisition and storage of the data by a vector which includes the polar scattering diagram and the light scattering, and the recognition phase, consisting acquisition of new data entry and finding the k nearest neighbors of this data entry, also determining the class of this vector in a supervised way. In order to validate this biometric methodology, we performed a cross-validated recognition task, and the results will be discussed in 4th part.

3. Experimentation

The device is tested on seven different subjects with different skin color, with apparent melanin concentration discrimination, as they are Caucasian to African, for the validation of the scattering spectrums. Via this protocol, the spectrums are obtained in Fig. 10, each point (lines) on these spectrum corresponds to the characteristic vectors which will be our training examples as the input of pattern recognition tool containing k-nearest neighbors (k-NN) statistical approach for classification and regression in learning algorithm. This learning algorithm contributes to the individual identification, namely recognition, by using data acquired by scattering spectrum.

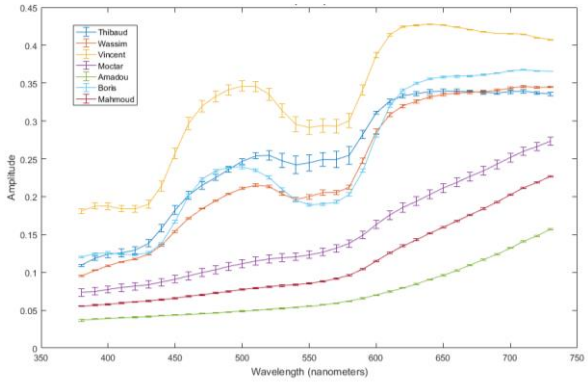

Fig. 10. Spectrum of skin samples acquired from right back of hand of each seven subjects

Besides, in order to observe variation of the spectrum due to the tissues humidity, measurement of dry and humidified skin for each 4 subjects is effectuated, using our system, as we can see in Fig. 11.

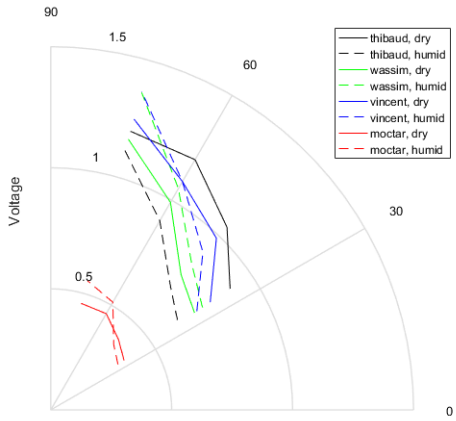

Fig. 11: Polar scattering diagram of subjects, full line representing dry measures, dashed line for humid measures. Humidification was applied by applying water on the back of hand, resulting of a fine water pellicle.

Finally, we feed the data in the recognition system, computing a cross-validated task, achieving up to 100% accuracy as we can see in the Fig. 12.

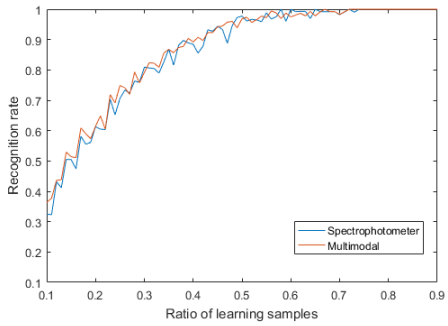

Fig. 12: Recognition rate for the two modalities of the recognition task. In blue, the recognition task was done with the spectrophotometer data, in red, all the data (with our system) was used. Only one angle is used in the algorithm.

4. Discussion

Although the scattering through the skin is a discriminative for all the wavelengths measured with spectrometer, Fig. 10 distinguish the samples of each seven subjects.

The standard deviation of the mean values for each subject, is minor as the measurements are consistent from each other. This permits a perfect recognition in the classification system, achieving a recognition rate of 100%, when sufficient amount of data is used in the learning set, and because of the seven test subjects whose chromophores are adequately distinctive.

For the sensor system, adding this modality in the recognition process lead to an increased performance in classification process. However, the gain is not significant as showed in Fig. 10, due to lack of test subjects. The recognition system was made with data of one particular angle, corresponding to the specular angle as the adjacent angle formed in the system. Scalar-extracted feature causes a lack of dimensionality as it confirmed by recognition rates in Fig. 12.

The system is constraint to multiple limitations, as we measure the integration of the absorption spectrum of the skin, $\int S_E * S_S * S_R \, d\lambda$ where S_E, S_S, and S_R are respectively the spectrum of emission, diffusion and receiver, conditioned by the spectrums of emission and reception of the electromagnetic waves. Thus, the quantity of the complex molecules (mainly oxyhemoglobin, melanin and water) are correlated. Despite, we present a consequent portion of the skin (around 7cm²), averaging the oxyhemoglobin amount in the measurement, favoring the measurement of melanin, which humans used in order to discriminate the skin, in the visible spectrum.

However, the accuracy of the method is adequately efficient on this protocol to identify the subjects, validating the biometric application of this methodology.

5. Conclusion

Skin recognition system is presented using a spectrometer in order to obtain input data as scattering diagrams due to the skin components, for learning algorithm which provides individual detection, reaching 100% accuracy with seven test subjects. The improvements in skin recognition may be used in medicine as a pathology detector instead of biopsy procedure, in cosmetology in order to observe reaction of chemical components on the skin, in computer graphics for animation, photorealistic rendering as well as in biometrics in order to individual detection.

6. Perspectives

Our perspective contains improvements for the optical system, acquisition, and augmented accuracy in algorithm with higher accuracy which requires higher number of training examples also a better clustering.

Training samples implies the accuracy of the learning algorithm. In our case, the input data of learning algorithm acquired from a system containing a LED. A monochromator could be used in order to generate a narrow spectrum, the input data for recognition tool would have greater dimensionality, providing better individual clustering with more training data. The monochromator can sweep its functional wavelength in order to make a spectrum of multiple wavelengths.

As described in the last paragraph, we could have a spectrum for each angle of measurement. This can be done also with a diffraction grating, that we could set up near the optics of camera filming the scene, in order to collect diffraction of the light by the skin.

The system is using a photodiode as the sensor, leading to different kind of noises, as the direct current noise of the power supply, or the electronic noise of the sensor. The noise could be filtered and amplified in a fashionable way to maximize the signal-to-noise ratio of the filtered signal, minimizing the standard deviation of multiple measurements.

In order to compensate the lack of dimensionality in the recognition system, the diffusion diagram would be used as input as well as in Fig. 11. This will be presented during the project valorization process, as the team is preparing a demonstrative system instead of the prototype used to gather the data presented in this article.

Another improvement for the recognition tool would be provided by coupling the system with a camera, which increase the quality of input data (binning methods) for a better clustering, and could be used to analyze the veins as the spatial arrangement of local distribution of the oxy-hemoglobin. Thus, it would be adequately distincitive to characterize a person, like in wide range of biometric solution.

Another perspective related to the training example is the determination of the study field. For instance, in order to adapt this device into medical field, the pathological samples would be needed as input of learning algorithm in order to make a pathological recognition tool. Another constraint comes from medical regulation which evaluate the device as well as its software as a medical device. Hence, in order to make a medical device to detect skin pathologies, this non-invasive device would be a class I medical device due to CE regulation and its software would reach certain accuracy for certain number of test.

7. Acknowledgements

First and foremost, the team wants to express gratitude to our supervisor Mr Stéphane Holé for the useful remarks, comments and engagement through the process of this project. We would also like to show gratitude to the committee, including Ms Catherine Achard, Mr Bruno Gas and Mr Sylvain Argentieri. Next, we want to thank Mr Jean-Charles Merton, and all the attendants who contributed to the project. Also, we like to thank all the subject who participated in the experience. Last but not least, we express sincere gratitude to our fellow classmates, Ms Gizem Temiz, Mr Amine Benamara, Mr Hassan Ait-Brik and Mr Rémi David-Le Guillou, who contributed a lot in this project.

8. References

[1] J. K. Wagner, C. Jovel, H. L. Norton, E. J. Parra, and M. D. Shriver, “Comparing quantitative measures of erythema, pigmentation and skin response using reflectometry,” *Pigment Cell Res.*, vol. 15, no. 5, pp. 379–384, Oct. 2002.

[2] N. Kollias and A. Baqer, “Spectroscopic characteristics of human melanin in vivo,” *J. Invest. Dermatol.*, vol. 85, no. 1, pp. 38–42, Jul. 1985.

[3] K. S. Bersha, “Spectral imaging and analysis of human skin,” University of Eastern Finland, 2010.

[4] M. Ferguson-Pell and S. Hagisawa, “An empirical technique to compensate for melanin when monitoring skin microcirculation using reflectance spectrophotometry,” *Med. Eng. Phys.*, vol. 17, no. 2, pp. 104–110, Mar. 1995.

[5] J. J. Riesz, *The spectroscopic properties of melanin*. University of Queensland, 2007.

[6] I. V. Meglinsky and S. J. Matcher, “Modelling the sampling volume for skin blood oxygenation measurements,” *ResearchGate*, vol. 39, no. 1, pp. 44–50, Feb. 2001.

[7] H. Gesche, D. Grosskurth, G. Küchler, and A. Patzak, “Continuous blood pressure measurement by using the pulse transit time: comparison to a cuff-based method,” *Eur. J. Appl. Physiol.*, vol. 112, no. 1, pp. 309–315, Jan. 2012.

[8] E. Angelopoulou, “Understanding the color of human skin,” 2001, vol. 4299, pp. 243–251.

[9] I. V. Meglinski and S. J. Matcher, “Computer simulation of the skin reflectance spectra", vol. 70, no. 2, pp. 179–86, Mar. 2003.

[10] A. Garcia-Uribe, J. Zou, M. Duvic, J. H. Cho-Vega, V. G. Prieto, and L. V. Wang, “In vivo diagnosis of melanoma and non-melanoma skin cancer using oblique incidence diffuse reflectance spectrometry,” *Cancer Res.*, vol. 72, no. 11, pp. 2738–2745, Jun. 2012.

[11] R. R. Anderson and J. A. Parrish, “The Optics of Human Skin,” *J. Invest. Dermatol.*, vol. 77, no. 1, pp. 13–19, Jul. 1981.

[12] J. Y. Qu, H. Chang, and S. Xiong, “Fluorescence spectral imaging for characterization of tissue based on multivariate statistical analysis,” *JOSA A*, vol. 19, no. 9, pp. 1823–1831, Sep. 2002.

[13] A. J. Thody, E. M. Higgins, K. Wakamatsu, S. Ito, S. A. Burchill, and J. M. Marks, “Pheomelanin as well as eumelanin is present in human epidermis,” *J. Invest. Dermatol.*, vol. 97, no. 2, pp. 340–344, Aug. 1991.

[14] G. Zonios, J. Bykowski, and N. Kollias, “Skin melanin, hemoglobin, and light scattering properties can be quantitatively assessed in vivo using diffuse reflectance spectroscopy,” *J. Invest. Dermatol.*, vol. 117, no. 6, pp. 1452–1457, Dec. 2001.

[15] J.-R. Kuo, M.-H. Chang, C.-C. Wang, C.-C. Chio, J.-J. Wang, and B.-S. Lin, “Wireless near-infrared spectroscopy system for determining brain hemoglobin levels in laboratory animals,” *J. Neurosci. Methods*, vol. 214, no. 2, pp. 204–209, Apr. 2013.

[16] F. Scholkmann *et al.*, “A review on continuous wave functional near-infrared spectroscopy and imaging instrumentation and methodology,” *NeuroImage*, vol. 85, pp. 6–27, Jan. 2014.

[17] I. V. Meglinski and S. J. Matcher, “Quantitative assessment of skin layers absorption and skin reflectance spectra simulation”, vol. 23, no. 4, pp. 741–53, Dec. 2002.

[18] C. Bordier, “Diffusion de la lumière par des tissus biologiques: Etude expérimentale et modélisation par l’équation de transfert radiatif vectorielle.,” Université Paris 6, 2009.

[19] W. G. Zijlstra, A. Buursma, and O. W. van Assendelft, *Visible and Near Infrared Absorption Spectra of Human and Animal Haemoglobin: Determination and Application*. VSP, 2000.
[20] "MEDICAL AND AESTHETIC LASERS: Semiconductor diode laser advances enable medical applications." [Online]. Available: http://www.bioopticsworld.com/articles/print/volume-7/issue-5/features/medical-and-aesthetic-lasers-semiconductor-diode-laser-advances-enable-medical-applications.html.
[21] A. Dubois, "Cours de biophotonique."
[22] L. Rossi, "Polarisation par diffusion." [Online]. Available: http://sesp.esep.pro/fr/pages_polarisation/polarisation-diffusion_impression.html.
[23] Sharayanan, *English: Depiction of Mie scattering on a spheric particle. The graph roughly displays scattering intensity per direction. From left to right : Rayleigh, intermediate and full Mie scattering.* 2007.
[24] T. Vo-Dinh, *Biomedical Photonics Handbook*. CRC Press, 2003.
[25] G. Yu, K. Pakbaz, and A. J. Heeger, "Semiconducting polymer diodes: Large size, low cost photodetectors with excellent visible-ultraviolet sensitivity," *Appl. Phys. Lett.*, vol. 64, no. 25, pp. 3422–3424, Jun. 1994.
[26] R. Korde and J. Geist, "Quantum efficiency stability of silicon photodiodes," *Appl. Opt.*, vol. 26, no. 24, pp. 5284–5290, Dec. 1987.
[27] E. R. Fossum and D. B. Hondongwa, "A Review of the Pinned Photodiode for CCD and CMOS Image Sensors," *IEEE J. Electron Devices Soc.*, vol. 2, no. 3, pp. 33–43, May 2014.
[28] K. L. Clarkson, "Fast algorithms for the all nearest neighbors problem," in *24th Annual Symposium on Foundations of Computer Science (sfcs 1983)*, 1983, pp. 226–232.